SUPPLEMENTARY MATERIAL: POLARIZATION DENOISING AND DEMOSAICKING: DATASET AND BASELINE METHOD

Muhamad Daniel Ariff Bin Abdul Rahman, Yusuke Monno, Masayuki Tanaka, and Masatoshi Okutomi

Institute of Science Tokyo, Japan

1. OVERVIEW

In this supplementary material, we provide more complete numerical and visual results, including the ones that are unable to be included in the main paper due to the page limit.

2. ADDITIONAL EXPERIMENTAL RESULTS

Tables 1, 2, and 3 show the quantitative comparisons for MPFA on the low, medium, and high noise-level conditions, respectively. From Table 1, we can see that IGRI-2→BM3D outperforms the other methods in the comparisons for I_0, I_{135}, and $S0$ and our method is the second best for those comparisons. In contrast, our method achieves the best results in the other evaluation categories. These results indicate that, for the low noise level, the noise does not much affect the performance of demosaicking, and consequently, demosaicking-then-denoising and denoising-then-demosaicking approaches reach similar performance. From Tables 2 and 3, we can see that our method outperforms all the other methods in all the evaluation categories.

Figures 1 and 2 show the visualization results for MPFA on the low, medium, and high noise-level conditions. We can see that our method performs better than the other methods for all three conditions in suppressing the noise, which can be confirmed by the AoP-DoP visualization results. For example, we can clearly see the characters in Figure 1 (middle) and Figure 2 (top and bottom).

Tables 4, 5, and 6 show the quantitative comparisons for CPFA on the low, medium, and high noise-level conditions, respectively. The overall trend is similar to the monochrome case, showing that IGRI-2→BM3D and our method demonstrate comparable performance for the low noise level and our method consistently provides the best performance for the medium and high noise levels.

Figures 3 and 4 show the visualization results for CPFA on the low, medium, and high noise-level conditions. Similar to the monochrome case, the AoP-DoP visualization results show clear differences between our method and the other methods on all the conditions. For example, we can clearly see that our method outperforms the others significantly in suppressing the noise in Color Checker and Alcohol Bin scenes in Figure 3 (top) and Figure 4 (top). Besides, we can clearly see the shape of the pot in Figure 3 (middle) for our method's result. Furthermore, we can clearly see the paprika in the AoP-DoP visualization for our method without significant noise in Figure 4 (bottom).

Given all of the numerical and the visual results, we can conclude that our method is the most stable and generally a better-performing method across a wide range of noise-level conditions.

Table 1: Quantitative comparison for MPFA on the low noise-level condition ($\sigma_G = 1.75$)

Method	PSNR ↑								Angle error ↓
	I_0	I_{45}	I_{90}	I_{135}	S_0	S_1	S_2	DoP	AoP
ICC [1]	40.27	39.33	40.47	39.23	43.43	44.83	43.01	32.10	31.61
IGRI-2 [2]	41.73	39.71	39.76	41.13	43.02	46.89	43.81	33.10	28.71
LPD [3]	39.22	38.58	39.31	38.75	44.35	41.56	40.52	28.36	23.74
ICC [1] → BM3D [4]	41.71	40.42	41.95	40.36	44.89	45.97	43.73	33.62	27.28
IGRI2 [2] → BM3D [4]	**43.44**	40.79	40.90	**42.70**	**45.10**	47.48	44.07	33.69	25.92
LPD [3] → BM3D [4]	39.26	38.60	39.39	38.78	44.17	41.79	40.65	28.53	22.97
PFCD → IGRI-2 (Ours)	42.97	**41.00**	**43.77**	41.10	44.92	**48.31**	**44.36**	**33.75**	**21.42**

Table 2: Quantitative comparison for MPFA on the medium noise-level condition ($\sigma_G = 4.29$)

Method	PSNR ↑								Angle error ↓
	I_0	I_{45}	I_{90}	I_{135}	S_0	S_1	S_2	DoP	AoP
ICC [1]	35.67	35.28	35.72	35.24	38.63	40.37	39.63	25.40	39.96
IGRI-2 [2]	36.10	35.39	35.39	35.91	37.42	42.87	41.31	27.94	37.56
LPD [3]	36.40	36.01	36.41	36.12	41.27	38.41	37.87	24.30	34.32
ICC [1] → BM3D [4]	39.13	38.29	39.20	38.29	42.55	43.08	41.78	30.02	36.04
IGRI-2 [2] → BM3D [4]	40.17	38.71	38.77	39.83	42.54	44.62	42.44	30.73	34.48
LPD [3] → BM3D [4]	37.47	36.97	37.50	37.13	42.61	39.46	38.78	25.64	32.38
PFCD → IGRI-2 (Ours)	**41.22**	**39.79**	**41.64**	**39.89**	**42.71**	**47.63**	**43.91**	**32.63**	**26.19**

Table 3: Quantitative comparison for MPFA on the high noise-level condition ($\sigma_G = 7.31$)

Method	PSNR ↑								Angle error ↓
	I_0	I_{45}	I_{90}	I_{135}	S_0	S_1	S_2	DoP	AoP
ICC [1]	32.07	31.89	32.06	31.81	34.94	36.95	36.50	23.74	43.95
IGRI-2 [2]	31.97	31.74	31.70	31.97	33.32	39.38	38.59	26.45	42.38
LPD [3]	31.98	31.80	31.96	31.82	37.31	33.53	33.31	20.46	41.86
ICC [1] → BM3D [4]	36.69	36.19	36.67	36.10	40.42	40.67	39.69	28.97	40.71
IGRI-2 [2] → BM3D [4]	37.41	36.70	36.68	37.37	40.36	41.96	40.61	30.13	39.72
LPD [3] → BM3D [4]	34.43	34.14	34.43	34.19	40.54	35.77	35.43	23.29	39.90
PFCD → IGRI-2 (Ours)	**40.01**	**38.90**	**40.09**	**38.96**	**41.18**	**47.13**	**43.69**	**34.31**	**30.24**

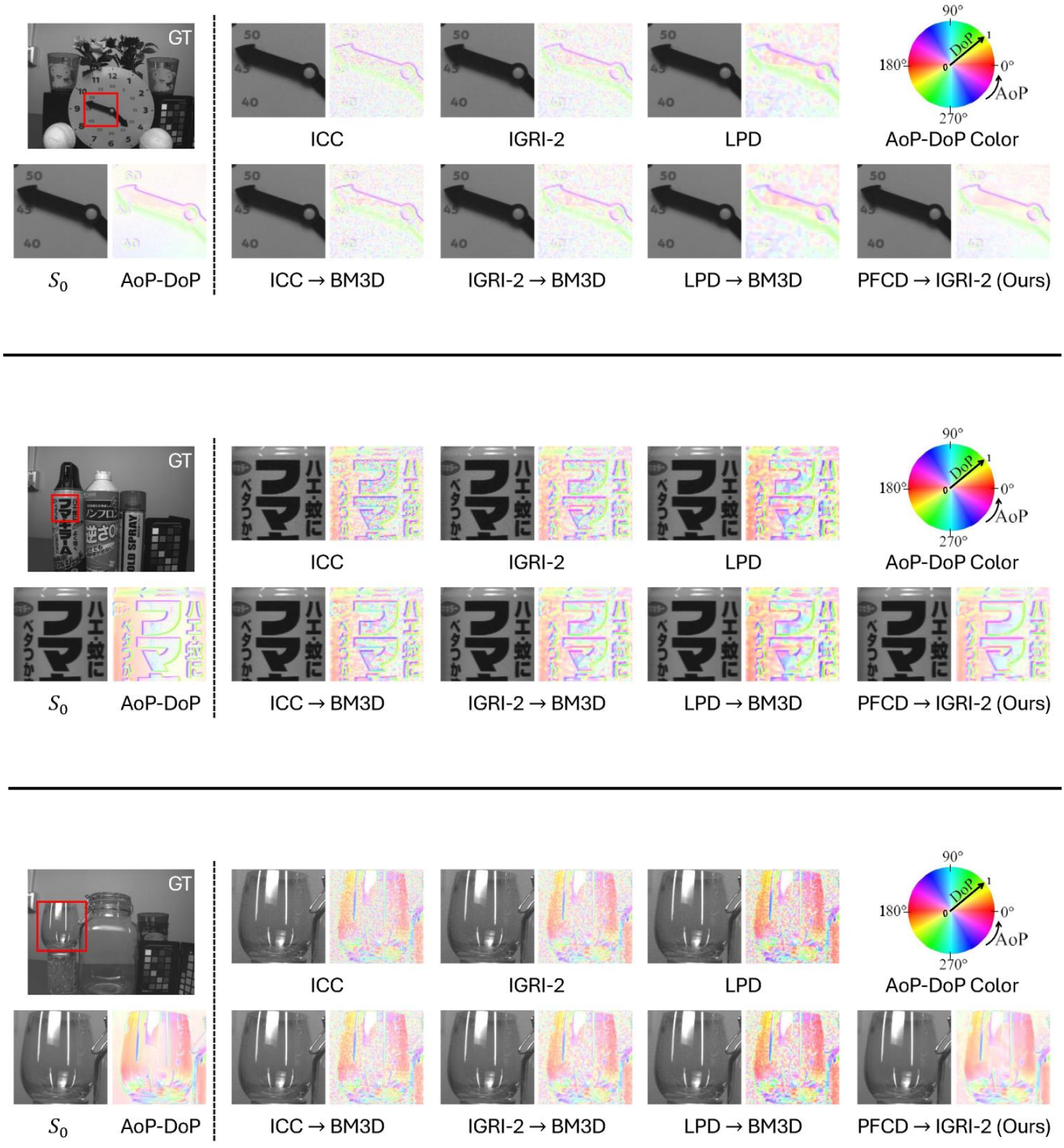

Fig. 1: Visual comparison for MPFA on the low (top), medium (middle), and high (bottom) noise-level conditions

Fig. 2: Visual comparison for MPFA on the low (top), medium (middle), and high (bottom) noise-level conditions

Table 4: Quantitative comparison for CPFA on the low noise-level Condition ($\sigma_R = 2.12, \sigma_G = 1.75, \sigma_B = 3.27$)

Method	CPSNR ↑								Angle error ↓
	I_0	I_{45}	I_{90}	I_{135}	S_0	S_1	S_2	DoP	AoP
IGRI-2 [2]	35.91	35.27	36.01	35.42	37.47	42.49	40.50	30.03	34.67
LPD [3]	34.35	33.74	34.15	33.91	35.71	40.79	39.00	27.31	29.82
JCPD [5]	35.25	34.94	35.69	34.72	36.44	42.42	40.77	29.83	37.26
IGRI-2 [2] → BM3D [4]	**36.60**	**35.87**	**36.71**	**36.05**	**38.22**	43.02	40.84	30.74	33.05
LPD [3] → BM3D [4]	34.37	33.76	34.19	33.93	35.69	40.96	39.10	27.48	29.25
JCPD [5] → BM3D	35.96	35.56	36.41	35.35	37.23	43.41	40.99	30.49	34.94
PFCD → IGRI-2 (Ours)	36.52	35.81	36.68	35.99	37.91	**43.53**	**41.12**	**31.18**	**28.87**

Table 5: Quantitative comparison for CPFA on the medium noise-level condition ($\sigma_R = 5.16, \sigma_G = 4.29, \sigma_B = 9.08$)

Method	CPSNR ↑								Angle error ↓
	I_0	I_{45}	I_{90}	I_{135}	S_0	S_1	S_2	DoP	AoP
IGRI-2 [2]	32.17	31.84	32.19	31.89	34.28	37.97	37.07	23.00	42.04
LPD [3]	32.24	31.83	32.15	31.93	33.94	37.38	36.38	22.67	36.05
JCPD [5]	30.86	30.75	31.12	30.54	31.57	38.19	37.91	23.47	43.55
IGRI-2 [2] → BM3D [4]	34.11	33.65	34.14	33.74	35.68	39.22	38.07	25.16	40.67
LPD [3] → BM3D [4]	32.66	32.22	32.58	32.34	34.32	37.98	36.85	23.54	35.26
JCPD [5] → BM3D	32.78	32.57	33.06	32.34	33.62	40.47	38.67	25.61	41.62
PFCD → IGRI-2 (Ours)	**34.94**	**34.42**	**34.99**	**34.54**	**36.36**	**42.00**	**40.08**	**28.96**	**34.52**

Table 6: Quantitative comparison for CPFA on the high noise-level condition ($\sigma_R = 8.62, \sigma_G = 7.31, \sigma_B = 15.79$)

Method	CPSNR ↑								Angle error ↓
	I_0	I_{45}	I_{90}	I_{135}	S_0	S_1	S_2	DoP	AoP
IGRI-2 [2]	28.75	28.59	28.71	28.57	31.13	34.22	33.82	20.96	45.55
LPD [3]	29.22	28.99	29.15	29.00	31.49	33.12	32.67	19.87	41.90
JCPD [5]	27.18	27.15	27.37	26.96	27.72	35.03	34.71	21.52	46.58
IGRI-2 [2] → BM3D [4]	31.52	31.26	31.48	31.25	34.92	35.86	35.29	23.42	44.49
LPD [3] → BM3D [4]	30.18	29.91	30.12	29.93	32.49	34.08	33.55	21.20	41.05
JCPD [5] → BM3D [4]	29.76	29.66	29.94	29.42	30.41	36.82	36.01	23.86	45.10
PFCD → IGRI-2 (Ours)	**33.71**	**33.33**	**33.72**	**33.42**	**35.04**	**41.12**	**39.52**	**29.91**	**37.97**

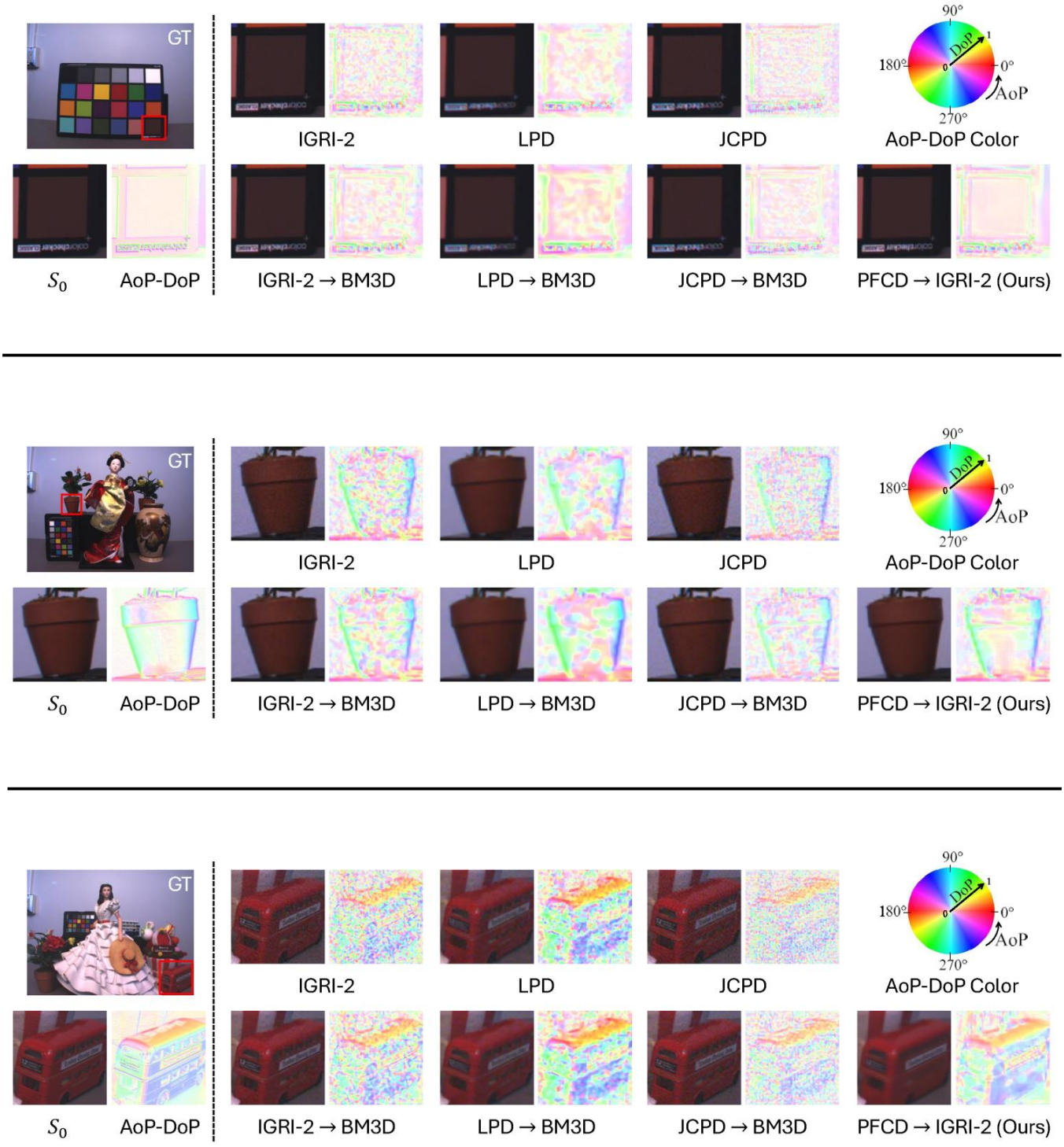

Fig. 3: Visual comparison for CPFA on the low (top), medium (middle), and high (bottom) noise-level conditions

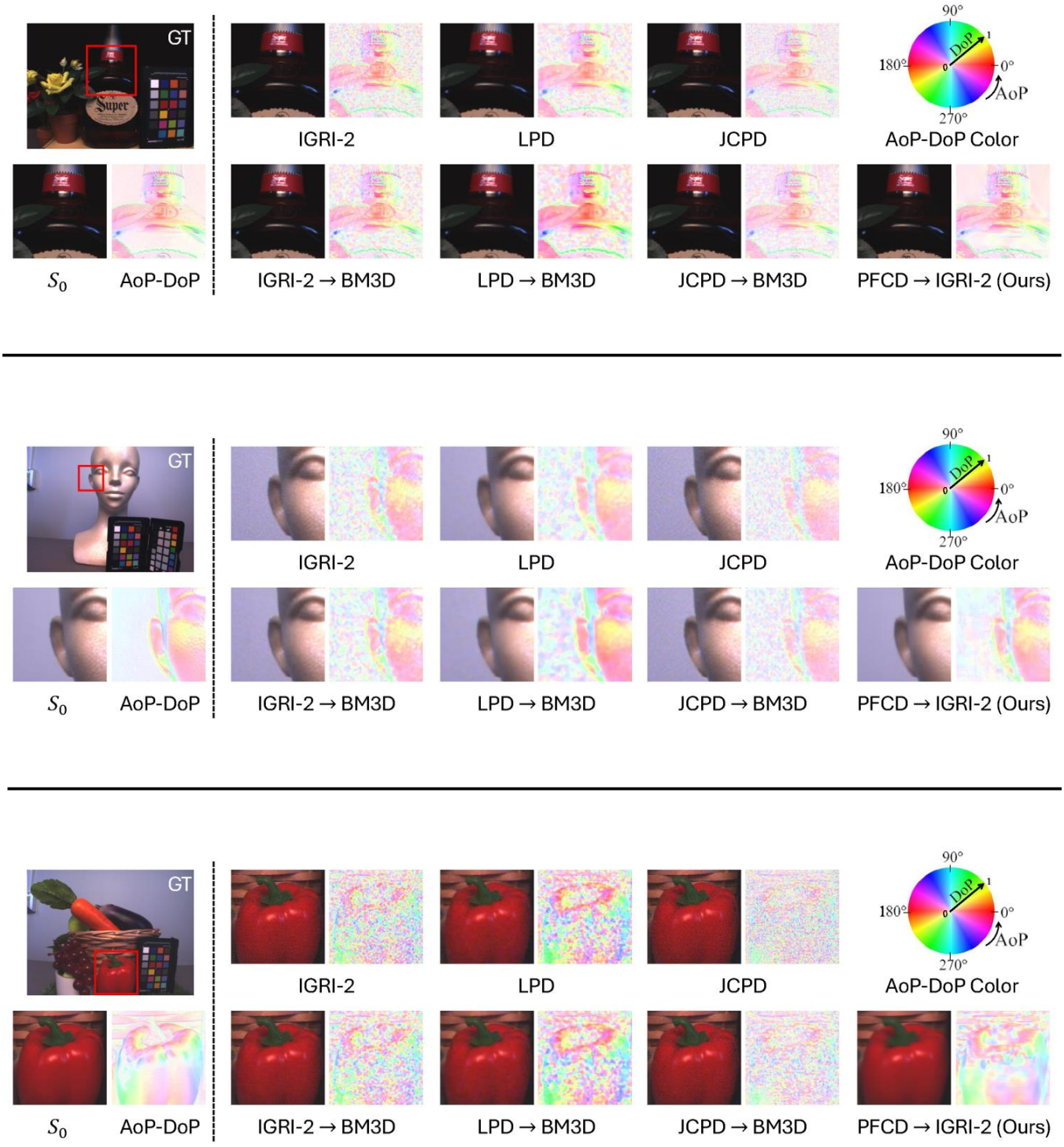

Fig. 4: Visual comparison for CPFA on the low (top), medium (middle), and high (bottom) noise-level conditions

3. REFERENCES

[1] Shumin Liu, Jiajia Chen, Yuan Xun, Xiaojin Zhao, and Chip-Hong Chang, "A new polarization image demosaicking algorithm by exploiting inter-channel correlations with guided filtering," *IEEE Transactions on Image Processing*, vol. 29, pp. 7076–7089, 2020.

[2] Miki Morimatsu, Yusuke Monno, Masayuki Tanaka, and Masatoshi Okutomi, "Monochrome and color polarization demosaicking based on intensity-guided residual interpolation," *IEEE Sensors Journal*, vol. 21, pp. 26985–26996, 2021.

[3] Simeng Qiu, Qiang Fu, Congli Wang, and Wolfgang Heidrich, "Linear polarization demosaicking for monochrome and colour polarization focal plane arrays," *Computer Graphics Forum*, vol. 40, pp. 77–89, 2021.

[4] Kostadin Dabov, Alessandro Foi, Vladimir Katkovnik, and Karen Egiazarian, "Image denoising by sparse 3-D transform-domain collaborative filtering," *IEEE Transactions on Image Processing*, vol. 16, no. 8, pp. 2080–2095, 2007.

[5] Sijia Wen, Yinqiang Zheng, and Feng Lu, "A sparse representation based joint demosaicing method for single-chip polarized color sensor," *IEEE Transactions on Image Processing*, vol. 30, pp. 4171–4182, 2021.